

Comparison of Transient Simulations on Overhead Cables by EMTP and FDTD

H. Xue, M. Natsui, A. Ametani, J. Mahseredjian, H. Tanaka, Y. Baba

Abstract--Transient simulations on an overhead cable are performed by an electromagnetic transient (EMT) analysis software and the finite-difference time-domain (FDTD) method. The differences between EMT-type simulations and FDTD computed results are investigated. It is made clear from the investigations that the EMT and FDTD approaches can give qualitatively the same results as far as appropriate models in each method are adopted. An influence of perfectly conducting earth and lossy earth on transient analysis is investigated using the FDTD method, and it is made clear that no accurate results can be obtained without proper earth modeling in FDTD.

Keywords: Electromagnetic Transient, overhead cable, EMTP, FDTD.

I. INTRODUCTION

EMT-type (electromagnetic transients) simulation tools based on transmission line (TL) theory and widely used all over the world and deemed to be accurate [1]-[5] for modern power systems. One of the significant advantages of the EMT approach is that the earth potential is zero, and thus the voltage of a conductor, is easily calculated as a voltage difference between the conductor and the earth. At the same time, when the effect of a lossy earth is to be considered in a transient simulation, the earth-return impedance and admittance formulas are necessary and are to be included in the conductor model. Especially, grounding of power equipment, such as the metallic sheath of a cable and lead wires connecting the equipment to the grounding electrode, become troublesome.

Numerical electromagnetic analysis (NEA) methods are becoming a powerful tool to study transient related phenomena in power systems [4]-[7]. The finite-difference time-domain (FDTD) method is widely used to simulate transient responses in time domain. FDTD can easily deal with a lossy earth, grounding, and mutual coupling between vertical and horizontal conductors. A significant advantage of FDTD is its capability for handling three-dimensional transients. However, it is not easy to calculate the voltage of a conductor by FDTD, because the earth is not at zero potential unless a perfectly conducting earth is assumed. Also, a circular cross-section

conductor is very hard to model in a FDTD simulation, since the basic element (called "cell") in FDTD simulations is in principle square-shaped.

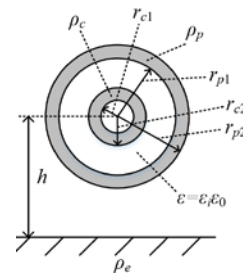
Considering the above facts, this paper performs transient simulations of switching surges on an overhead cable (overhead conductor and gas-insulated bus) which is part of a gas-insulated substation [8] by EMTP [2] and by FDTD [7].

In Section II, the modelling of a cable considering a lossy earth and a lead wire connecting the conductor to a source and to the earth are explained for both EMTP and FDTD. Also, a method to calculate the voltage on the conductor in FDTD simulations is described. In Section III, transient simulations of switching surges are performed by EMTP and FDTD. The simulation results by EMTP are compared with those by FDTD and the differences are investigated.

II. MODELING OF CIRCUIT ELEMENTS

A. EMTP

1) Overhead cable



$h = 0.5$ m, $r_{c1} = 3$ cm, $r_{c2} = 4$ cm, $r_{p1} = 13$ cm and $r_{p2} = 14$ cm, resistivities: core $\rho_c = 2.8 \times 10^{-8}$ Ω m, pipe $\rho_p = 2.8 \times 10^{-8}$ Ω m, earth $\rho_e = 100$ Ω m, relative permittivity: SF₆ gas $\epsilon_i = 1$

Fig. 1 Cross-section of a gas-insulated bus

Since the coaxial cable illustrated in Fig. 1 is composed of a core and a metallic sheath, the conductor internal impedance and admittance are given as a 2×2 matrix. The details of the matrix composition and related formulas are well described in [9]. For an overhead cable, earth-return impedance Z_e and space admittance Y_s are adopted [9].

2) Lead wire (vertical conductor)

The lead wire connecting the overhead cable to the earth is a vertical conductor, for which the surge impedance formula is given approximately by [10]

$$Z_{0v} = 60 \left[\ln \left(\frac{h}{r} \right) - 1 \right] \quad (1)$$

H. Xue, M. Natsui, A. Ametani and J. Mahseredjian are with Polytechnique Montreal, 2500, chemin de Polytechnique, Montréal (Québec) H3T1J4, Canada (e-mail: haoyan.xue@polymtl.ca, masashi.natsui@polymtl.ca, aametani@mail.doshisha.ac.jp, jeanm@polymtl.ca)

H. Tanaka and Y. Baba are with Doshisha University, Kyoto, 602-8580, Japan.

where h is conductor height and r is conductor radius.

3) Grounding

Modeling a grounding electrode installed in a lossy earth is very difficult in the TL approach, because the earth is at zero potential, i.e. the earth is a perfect grounding electrode. Thus, a similar approach for modeling a conductor above lossy earth is required [11], [12].

B. FDTD

1) Overhead cable

In FDTD simulations, the working space and media in the three dimensional (x, y, z axes) space are discretized with a cubic cell with the cell size Δs . Arbitrary resistivity and permeability of the conductor are easily modeled in FDTD simulations.

2) Earth

It is straightforward to model a lossy earth with resistivity ρ_e and relative permittivity ϵ_r in FDTD simulations. Also, a perfectly conducting earth is easily modeled.

3) Lead wire (vertical conductor)

In FDTD simulations, it is not a problem if a conductor is either horizontal or vertical to the earth surface. However, the cross-section area of the conductor causes a problem if it is smaller than the cross-section area Δs^2 of the cell adopted in the simulations. In such a case, a thin-wire model has to be used [6].

4) Grounding

When a lead wire is to be grounded (terminated) to a zero-potential earth surface in the same manner as in the TL approach, the earth is represented by a perfectly conducting earth in FDTD simulations. Then, the effect of a lossy earth cannot be considered in such simulations.

III. SIMULATION RESULTS AND DISCUSSION

To perform transient simulations with FDTD on the cable in Fig. 2 with the length $x=6$ m, the cell size is set to $\Delta s = 1$ cm to consider the pipe thickness of 1 cm.

A. Single Overhead Conductor

1) Model circuit

Fig. 2 illustrates a simple example for a comparison of transient simulations by EMTP and FDTD. The conductor with the length of $x=6$ m is composed of a core of the overhead cable illustrated in Fig. 1. The voltage source is represented as in Fig. 2 (b). A lead wire connects the sending end of the conductor to the source of which the other end is terminated at a zero potential earth. Since the conductor receiving end is open circuited, the modeling of the lead wire is necessary only at the sending end. In EMTP, the lead wire is represented as a constant-parameter distributed line with surge impedance Z_{0v} , calculated by (1): $Z_{0v} = 221.3 \Omega$ for $h=0.5$ m and $r=4.6$ mm. The propagation velocity c_v is assumed to be 280 m/ μ s [10]. When 300 m/ μ s is assumed, only a minor difference is observed in EMTP simulation

results. In the FDTD, the lead wire is easily modeled, but the grounding to a zero potential plane is troublesome. Thus, an ideal earth is assumed for the length of 2 m as in Fig. 3, and the lead wire is grounded to the ideal earth.

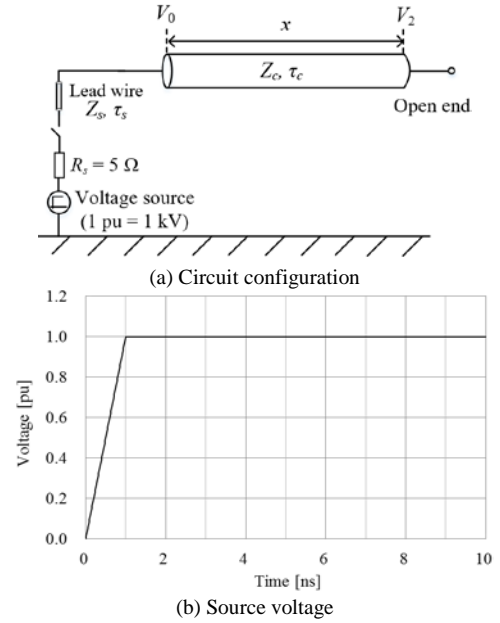


Fig. 2 Single conductor (core of Fig. 1)

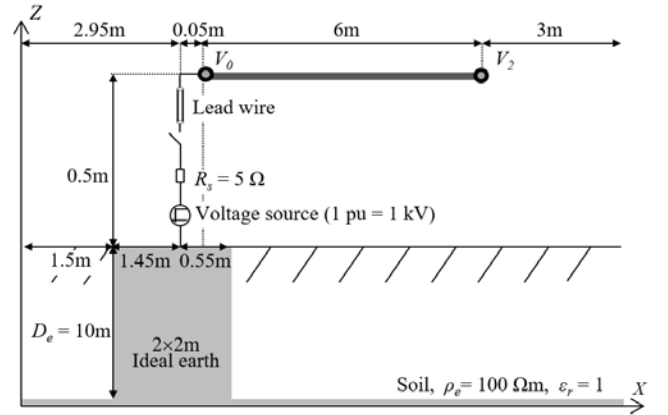


Fig. 3 Circuit configuration of FDTD

2) Simulation results for $\rho_e = 0 \Omega m$

Fig. 4 shows simulation results of transient voltages by EMTP and FDTD in the case of an ideal earth, i.e. $\rho_e = 0 \Omega m$.

A pulse-like voltage with a width of about 3.4 ns and voltage of about 0.9 pu is observed in the EMTP result of Fig. 4 (a), sending-end voltage V_0 . The voltage is produced by traveling wave reflection and refraction between the source grounding and the sending end of the conductor, i.e. the lead wire. Since the wire length is 0.5 m, the travel time, τ_s , is about 1.7 ns (two travel times give 3.4 ns). In the receiving-end voltage V_2 in Fig. 4 (b), the first traveling wave arrives at the receiving end at $t = \tau_c + \tau_s = 21.7$ ns, where $\tau_c = x/c = 6/0.3 = 20$ ns. The wave is reflected at the sending end and the source grounding, similarly to that in the sending-

end voltage. The analytical calculation of the voltages in Fig. 4 is described in Appendix.

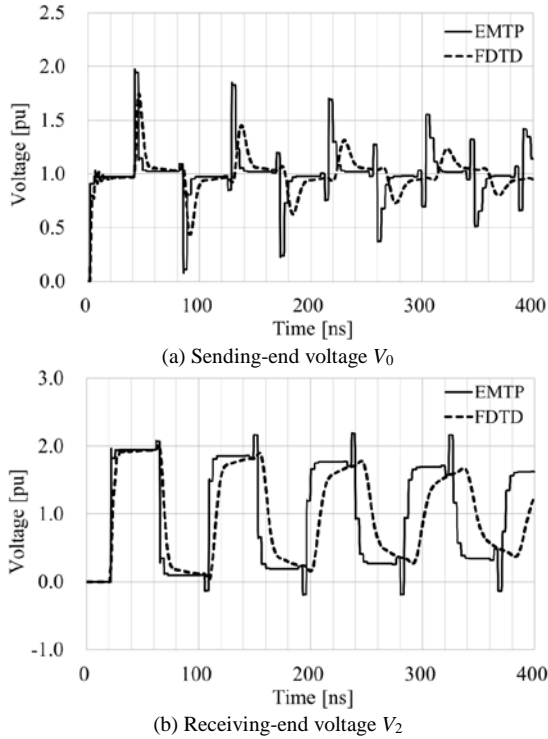


Fig. 4 Switching surges of a single conductor, $\rho_e = 0 \Omega m$

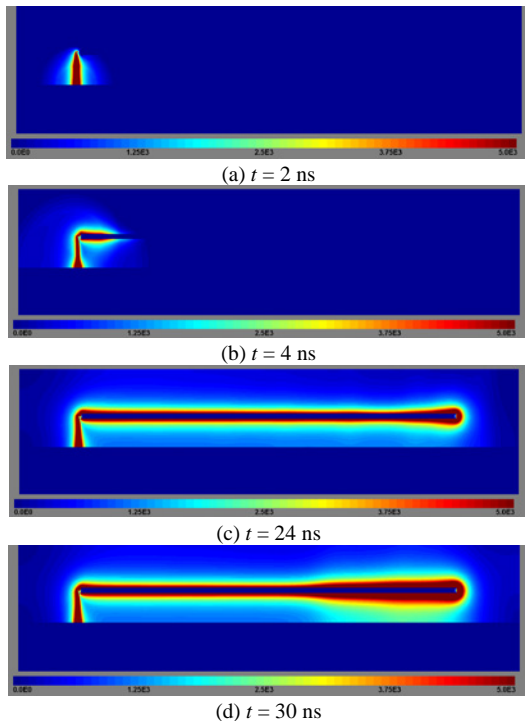


Fig. 5 Electric field intensity (1000 V/m = 1 pu) in cross-sectional view calculated by FDTD, $\rho_e = 0 \Omega m$

Fig. 5 shows the electric field intensity calculated with FDTD as a function of time within 30 ns. It is clear that the wave reaches the sending-end of the conductor at $t = 2$ ns. As time increases, i.e. $t = 24$ and 30 ns, the wave propagates to

the receiving-end of the conductor, and also reflects back to the source side. Because of reflection, the electric field intensity is clearly enlarged around the conductor.

3) Simulation results for $\rho_e = 100 \Omega m$

Fig. 3 shows the earth model and depth in the simulation of FDTD. The earth depth D_e is assumed to be 10 m, and there is a perfectly conducting earth at the bottom of the space. It is important to point that the earth model should have enough space to make the electric field intensity decay sufficiently and reach the zero potential level. Also, it has a perfectly conducting earth block below the lead wire because EMTP cannot consider a vertical conductor (lead wire) above a lossy earth.

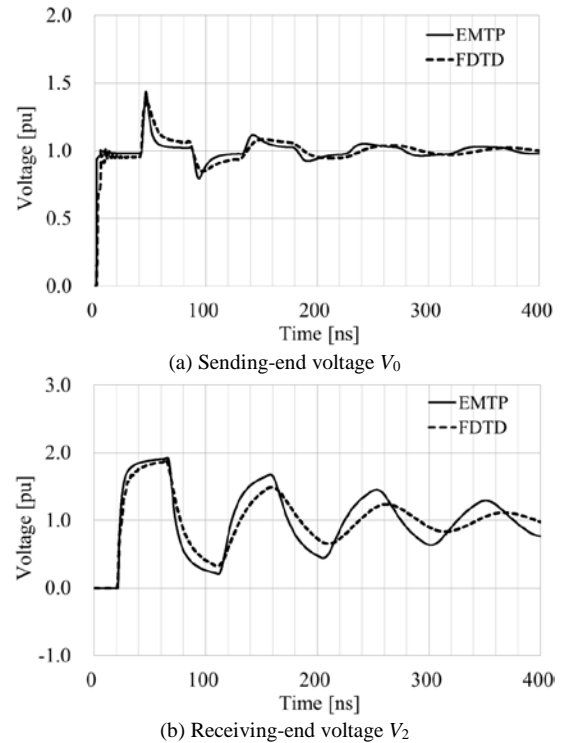


Fig. 6 Switching surges of a single conductor, $\rho_e = 100 \Omega m$

It is observed in Fig. 6 that the overall wave shapes of V_0 and V_2 calculated by EMTP and FDTD are similar. Because of lossy earth, the waveforms of Fig. 6 show a larger damping effect than Fig. 4. At the FDTD waveform of sending-end voltage V_0 in Fig. 6 (a), a stair-case voltage increase is observed. The voltage is estimated to be produced by the boundary of the perfectly conducting earth and the lossy earth in Fig. 3. Since the distance from the sending-end to the boundary is 0.55 m, the two travel time is about 3.5 ns which corresponds the time span of the stair-case like voltage.

4) Effect of earth depth

When the perfectly conducting earth is assumed, the electromagnetic field radiated from the conductor is completely reflected on the surface of the earth and no field distribution appears in the earth. Thus, the surge voltage is not affected by the depth of the earth. On the other hand, the

electromagnetic field penetrates into the earth in the case of lossy earth. Therefore, the effect of lossy earth should be dependent on the depth of the earth.

For estimating the penetration depth, the skin depth is generally assumed by the following equation

$$\delta = \sqrt{\frac{\rho_e}{\pi f \mu_0}} \quad (2)$$

In this study, the horizontal length of the conductor is 6 m and the propagation speed of the voltage on the conductor is assumed to be 300 m/ μ s. Therefore, considering the open-end condition of the conductor, the frequency is expected to be 12.5 MHz by dividing the speed by the quadruple length. A permeability of $4\pi \times 10^{-7}$ H/m (vacuum) and earth resistivity of 100 Ω m are also assumed. Thus, the skin depth δ is expected to be 1.42 m in this study.

Figs. 7, 8 and 9 show the switching surges for the earth depth of 0.5 m, 1.5 m and 3 m, respectively. For $D_e = 0.5$ m, which is the same as the height of the conductor, but less than the skin depth, the surge oscillation amplitude is larger than the result of EMTP. The amplitude decreases according to the increase of the earth depth. The waveform for $D_e = 1.5$ m, which is almost the same as the skin depth, can be said to be similar to the result of EMTP. For $D_e = 3$ m, which is around the double of the skin depth, the waveform almost converges and corresponds to the result for $D_e = 10$ m shown in Fig. 6.

These results clearly show that the idea of skin depth is useful to model a lossy earth in FDTD.

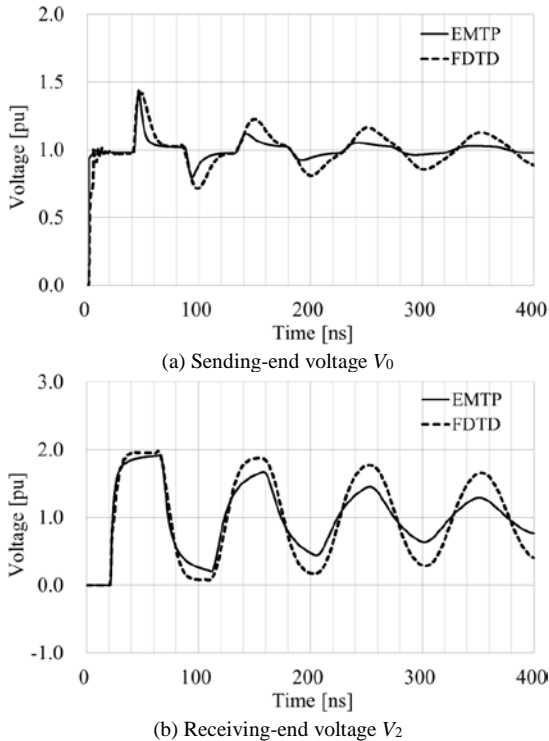


Fig. 7 Switching surges of a single conductor, $\rho_e = 100 \Omega$ m, $D_e = 0.5$ m.

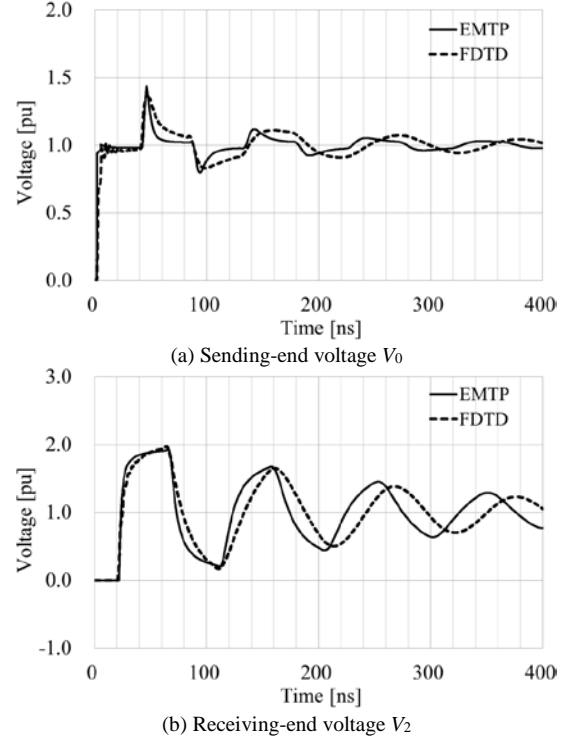


Fig. 8 Switching surges of a single conductor, $\rho_e = 100 \Omega$ m, $D_e = 1.5$ m.

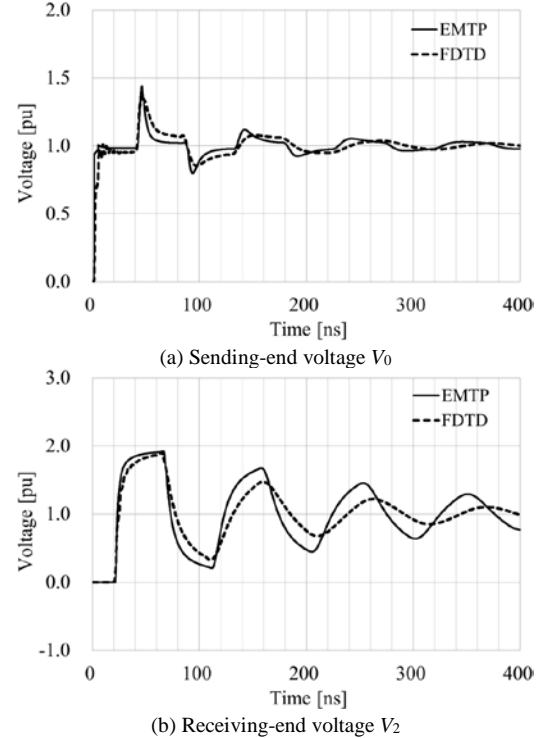


Fig. 9 Switching surges of a single conductor, $\rho_e = 100 \Omega$ m, $D_e = 3$ m.

B. Gas-Insulated Bus

1) Model circuit

Fig. 10 illustrates a Gas-Insulated Bus model circuit. There are three lead wires with lengths of 0.5 m and 0.36 m for connecting the source to the core sending-end, the pipe to

earth at $x = x_1 = 2$ m, and the pipe receiving-end to earth at $x = x_1 + x_2 = 6$ m.

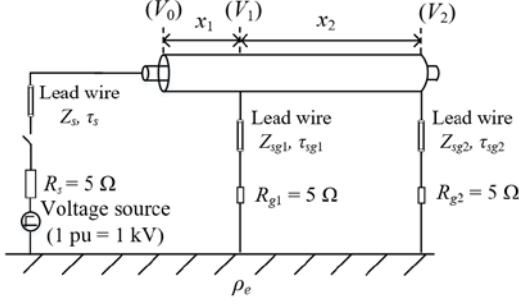


Fig. 10 Configuration of a cascaded GI Bus

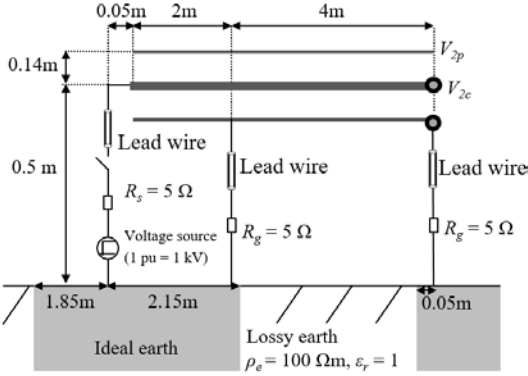
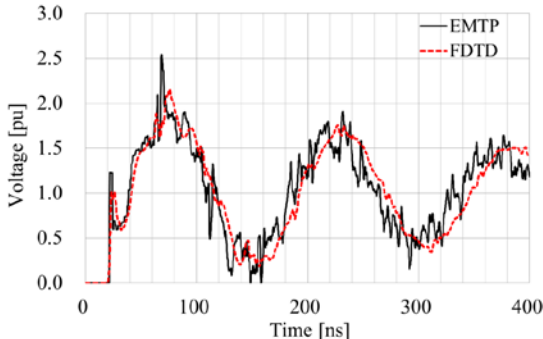


Fig. 11 A model circuit of GIB by FDTD

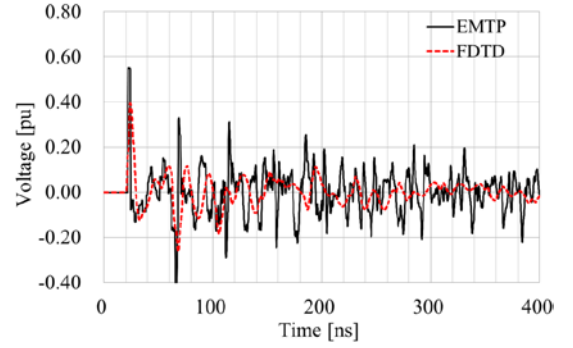
As indicated before, in FDTD, modeling of the lead wires is straightforward, but grounding the wires to earth is complicated. To solve this difficulty, a model circuit illustrated in Fig. 11, similarly to Fig. 3, is adopted in the FDTD. In Fig. 11, the lead wires are terminated on the ideal earth in the same manner as in EMTP.

2) Simulation results for $\rho_e = 0 \Omega\text{m}$

Fig. 12 shows simulation results of core and pipe voltages at the receiving-end with $\rho_e = 0 \Omega\text{m}$. It is clear that the result of EMTP qualitatively agrees with the result of FDTD for V_{2c} and V_{2p} . Also, the result of EMTP involves high frequency oscillations. On the contrary, the result of FDTD is more smooth due to the fact that high frequency components are damped by the radiation losses in the surrounding medium.



(a) Core voltage at receiving-end V_{2c}

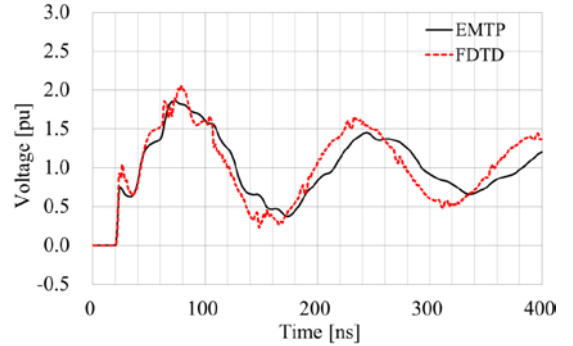


(b) Pipe voltage at receiving-end V_{2p}

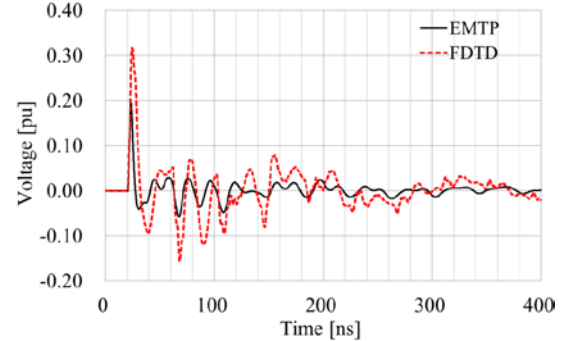
Fig. 12 Calculated core and pipe voltages at receiving-end, $\rho_e = 0 \Omega\text{m}$

3) Simulation results for $\rho_e = 100 \Omega\text{m}$

The simulated results of a lossy earth with EMTP and FDTD are shown and compared in Fig. 13. The high frequency components are much more damped in EMTP. When the lossy earth ($\rho_e = 100 \Omega\text{m}$) is considered, both EMTP and FDTD show a lower voltage than that in Fig. 12 in the case of an ideal earth, $\rho_e = 0$. Moreover, Fig. 13 (b) still includes a few high frequency oscillations for the results of EMTP and FDTD. Such oscillations can be the results of reflections and refractions at the different boundaries of lead wires. It is clear that the results of EMTP have the smallest values for the first peak of V_{2c} and V_{2p} . After first a few cycles, the waveform of EMTP agrees qualitatively with FDTD.



(a) Core voltage at receiving-end V_{2c}



(b) Pipe voltage at receiving-end V_{2p}

Fig. 13 Calculated core and pipe voltages at receiving-end, $\rho_e = 100 \Omega\text{m}$

IV. CONCLUSION

This paper has discussed transient simulations on an overhead line and gas-insulated bus (overhead cable) by EMTP and FDTD. It is found that FDTD computed results

agree reasonably well with EMTP simulation results as far as proper modeling methods are adopted in EMTP and FDTD. It has been made clear that the modeling of earth (depth and width) in FDTD simulation affects significantly the computed results, and the earth depth should be set to be more than two times the penetration depth at the dominant frequency of the transient. Vertical lead wires for connecting a source to a core conductor and for pipe grounding, influence significantly EMTP simulation results, when those are represented as a distributed-parameter line model.

One of the main advantages of FDTD is that a three-dimensional transient is easily handled. However, required computer resources (CPU time and memory) become very large. Each FDTD computation requires about 5 hours of CPU time.

V. APPENDIX

The analytical calculation of switching surge on a single conductor is given here.

At 20 MHz

$$Z_s = 60 \left[\ln \left(\frac{h}{r} \right) - 1 \right] = 221.3 \Omega \quad (\text{A.1})$$

$$Z_c = R_r = 193.1 \Omega \quad (\text{A.2})$$

$$(1) \quad t_1 = \tau_s = 1.7 \text{ ns}, \quad E_0 = 1 \text{ pu}$$

$$\lambda_{s0} = \frac{2Z_c}{Z_s + Z_c} = \frac{2 \times 193.1}{221.3 + 193.1} = 0.932$$

$$V_0 = \lambda_{s0} E_0 = 0.932 \text{ pu} = E_{02} \quad (\text{A.3})$$

$$(2) \text{ Negative reflection at the earth surface (or } R_s = 5 \Omega):$$

$$E_{0s} = V_0 - E_0 = -0.068 \text{ pu}$$

$$t_1' = t_1 + 2\tau_s = 5.1 \text{ ns:}$$

$$V_0(t_1') = V_0(t_1) - \lambda_{s0} E_{0s} = 0.932 + 0.0634 = 0.9954 \text{ pu} \quad (\text{A.4})$$

Z_c might be higher than 193.1Ω because the frequency is already lower than 20 MHz at this time period.

$$(3) \quad t_2 = \tau_s + \tau_c = 21.7 \text{ ns}, \quad E_{2f} = E_{02}(\tau_c) = 0.932 \text{ pu}$$

Receiving-end open

$$\lambda_{2f} = 2, \quad \therefore V_2 = 2E_{2f} = 1.864 \text{ pu} \quad (\text{A.5})$$

$$(4) \quad t_3 = t_2 + \tau_c = \tau_s + 2\tau_c = 41.7 \text{ ns}, \quad E_{0b} = E_{2b}(\tau_c)$$

$$\lambda_{0b} = \frac{2Z_s}{Z_s + Z_c} = \frac{2 \times 221.3}{221.3 + 193.1} = \frac{442.6}{414.4} = 1.07$$

$$\therefore V_0 = V_0(t_1) + \lambda_{0b} E_{0b} = 0.932 + 1.07 \times 0.932 = 1.93 \text{ pu} \quad (\text{A.6})$$

$$(5) \text{ Negative reflection: } E_{0s} = V_0 - E_0 = 1.93 - 1 = 0.93 \text{ pu}$$

$$t_3' = t_3 + 2\tau_s = 45.1 \text{ ns:}$$

$$V_0(t_3') = V_0(t_3) - \lambda_{s0} E_{0s} = 1.93 - 0.87 = 1.06 \text{ pu} \quad (\text{A.7})$$

The above analysis explains the pulse-like voltage of V_0 observed in Fig. 4 (a) at $t = 40 \text{ ns}$ with width 3.4 ns and

voltage about 0.9 pu, i.e. the pulse-like voltage is produced by the source lead wire with length 0.5 m.

VI. REFERENCES

- [1] H. W. Dommel, *Electromagnetic Transients Program (EMTP) Theory Book*, Portland: BPA, 1986.
- [2] J. Mahseredjian, S. Denetière, L. Dubé, B. Khodabakhchian and L. Gérin-Lajoie, "On a new approach for the simulation of transients in power systems," *Electric Power Systems Research*, Vol. 77, Issue 11, September 2007, pp. 1514-1520.
- [3] J. Mahseredjian, V. Dinavahi and J.A. Martinez "Simulation Tools for Electromagnetic Transients in Power Systems: Overview and Challenges", *IEEE Transactions on Power Delivery*, Vol. 24, Issue 3, pp. 1657-1669, July 2009
- [4] A. Ametani (Editor), *Numerical Analysis of Power System Transients and Dynamics*, London: IET Press, 2015.
- [5] A. Ametani, N. Nagaoka, Y. Baba and T. Ohno, *Power System Transients: Theory and Applications*, New York: CRC Press, 2014.
- [6] CIGRE WG C4.501, "Guideline for numerical electromagnetic analysis method and Its application to surge phenomena", CIGRE TB-543, 2013
- [7] Central Research Institute of Electric Power Industries, Virtual Surge Test Lab. (VSTL), <http://criepi.denken.or.jp/>, July 2007.
- [8] A. Ametani, T. Goto, N. Nagaoka and H. Omura, "Induced surge characteristics on a control cable in a gas-insulated substation due to switching operation," *IEEJ Trans. Power and Energy*, vol. 127, pp. 1306-1312, 2007.
- [9] A. Ametani, "A general formulation of impedance and admittance of cables," *IEEE Trans. Power Appar. Syst.*, vol. 99, pp. 902-910, 1980.
- [10] A. Ametani, Y. Kasai, J. Sawada, A. Mochizuki and T. Yamada "Frequency-dependent impedance of vertical conductors and a multiconductor tower model," *Proc. IEE*, vol. 141, pp. 339-345, 1994.
- [11] E. D. Sunde, *Earth conduction effects in transmission systems*, New York: Dover, 1968.
- [12] A. Ametani, D. Soyama, Y. Ishibashi, N. Nagaoka and S. Okabe, "Modeling of a buried conductor for an electromagnetic transient simulation," *IEEJ Trans. EEE*, vol. 1, pp. 45-55, 2006.